J. Fluid Mech. (1978), *vol.* 87, *part* 1, *pp.* 1–16
Printed in Great Britain

The steady flow of closely fitting incompressible elastic spheres in a tube

By HÜSNÜ TÖZEREN AND RICHARD SKALAK
Department of Civil Engineering and Engineering Mechanics, Columbia University, New York 10027

(Received 27 August 1977)

The steady flow of a suspension of closely fitting, neutrally buoyant, incompressible and elastic spheres through a circular cylindrical tube is investigated under the assumption that lubrication theory is valid in the fluid region. A series solution giving the displacement field of an elastic incompressible sphere under axisymmetrically distributed surface tractions is developed. It is found that, for closely fitting particles, flow properties of the suspension are strongly dependent on the shear modulus of the elastic material and the velocity of the particle.

1. Introduction

The steady flow of a suspension of neutrally buoyant particles through a circular cylindrical tube has been extensively considered as a model of capillary blood flow. Rigid particles of many different shapes have been used to model the blood cells, e.g. spherical particles (Wang & Skalak 1969; Hochmuth & Sutera 1970; Bungay & Brenner 1973), spheroids (Chen & Skalak 1970), flat disks (Bugliarello & Hsaio 1967; Lew & Fung 1969; Aroesty & Gross 1970) and particles shaped like red blood cells (Skalak, Chen & Chien 1972). Experimental studies concerning the flow behaviour of a variety of rigid models are also available, including disks, diskoids, spherical caps and particles shaped like red cells (Sutera & Hochmuth 1968; Hochmuth & Sutera 1970).

In recent years intensive theoretical and experimental research has been directed towards the determination of mechanical properties of the constituents of blood and the study of flow properties of suspensions of flexible particles (Sutera, Seshadri & Hochmuth 1970; Cokelet 1976). Current developments in the understanding of material properties of blood cells have led to the formulation of more complex theoretical models for the blood cells. The motion of neutrally buoyant liquid drops with surface tension has been investigated by Hyman & Skalak (1972). Lighthill (1968) and Fitz-Gerald (1969) applied lubrication theory to analyse the axisymmetric flow of neutrally buoyant compressible particles in fluid-filled tubes. They assumed that for any particle there exists a reference pressure such that the particle has the same diameter as the tube when this reference pressure is uniformly applied. Moreover these compressible particles undergo radial (in the sense of cylindrical co-ordinates) deflexions proportional to the amount by which the local lubrication pressures exceed the reference pressures. A more realistic representation of a red blood cell as an elastic shell filled with an incompressible, viscous fluid has been developed by Zarda, Chien & Skalak

(1977*a*). The capillary flow problem for this model is given by Zarda, Chien & Skalak (1977*b*).

This paper investigates the steady motion of an elastic incompressible sphere through a circular cylindrical tube filled with viscous fluid. This study was originally motivated by an interest in the flow of white blood cells in narrow capillary blood vessels (see Bagge 1975). However, the theory may be applicable also to some other systems involving particle–fluid interactions, such as the motion of red blood cells in narrow capillaries and transport of encapsulated solid matter in pipelines. In such cases, the present model may serve as a qualitative guide to the nature of results to be expected.

The present theory is different from the previous theories of Lighthill (1968) and Fitz-Gerald (1969) in several ways and hence not directly comparable. First, the particle is considered as a three-dimensional elastic continuum in the present treatment rather than as an isolated response to the local pressure. Second, the incompressible elastic particles treated herein do not deflect in any way under any uniform reference pressure. There are also important differences in the form of the equation expressing the condition of zero net drag on the particle. Lighthill (1968) and Fitz-Gerald (1969) assumed that the force due to the pressure drop across the particle is approximately equal to the resultant of shear stresses acting along the surface of the particle. It will be shown in §3 by the use of singular perturbation expansions derived by Bungay & Brenner (1973) for closely fitting rigid spheres that this assumption leads to substantial errors in the evaluation of the pressure drop across the particle.

The suspending fluid in the present treatment is assumed to be incompressible and Newtonian. The Reynolds number in the microcirculation is typically of the order of 10^{-3}. Hence the fluid inertial terms are neglected. Further, it is assumed that the clearance between the cell and the capillary walls is sufficiently small that lubrication theory may be applied. Lubrication theory is known to give accurate results for closely fitting rigid particles (Skalak *et al.* 1972).

There is an extensive literature on the theory of linear elasticity concerning the equilibrium and vibrations of elastic spheres (Love 1944). The general solution to the equations of equilibrium of an incompressible elastic medium in spherical co-ordinates is given by Lamb (1945). In the present treatment, Lamb's general solution is employed to obtain the displacement field of an elastic incompressible sphere when arbitrary axisymmetric stress distributions are specified along the boundary.

The derivation of the series solution for the displacement field of an elastic incompressible sphere under axisymmetric surface tractions and the lubrication-theory equations are given in §2. In §3 the present model is compared with the previous theories of Lighthill (1968) and Fitz-Gerald (1969) and the numerical results are discussed in §4.

2. Formulation

Consider an elastic incompressible particle of initially spherical shape moving axisymmetrically with a uniform velocity U through a fluid-filled circular cylindrical tube of radius r_0. The initial radius a of the particle is supposed to be comparable with or slightly greater than the radius of the cylindrical tube. The suspending fluid is assumed to be incompressible and Newtonian with uniform viscosity μ and uniform density ρ, which is taken to be equal to the density of the particle. The mean velocity V of the suspension is assumed to be maintained at a constant value by the application of a constant pressure difference Δp over some length including the particle.

The inertial terms are neglected in the Navier–Stokes equations and the motion of the suspending fluid is considered to be a steady Stokes flow relative to the particle. The equations of Stokes flow are

$$\mu \nabla^2 \mathbf{v} = \nabla p_f, \tag{2.1}$$

where $\mathbf{v}$ is the velocity vector and p_f is the pressure in the fluid region. Subscripts f and s are used to identify the variables in the fluid and solid regions respectively. The equation of continuity is

$$\nabla . \mathbf{v} = 0. \tag{2.2}$$

The clearance between the particle and the circular tube is assumed to be sufficiently small that lubrication theory may be applied. Under these assumptions the equations of motion (2.1) and continuity (2.2) reduce to the Reynolds equation of lubrication theory. When referred to the cylindrical co-ordinate system (R, ϕ, Z) fixed to the centre of the particle (Fitz-Gerald 1969), this Reynolds equation is

$$\frac{dp_f}{dz} = \left[r_0 Q - U\left(\tfrac{1}{2}r_0^2 + \frac{2r_0 h - h^2}{4\ln(1-h/r_0)}\right)\right]\left[\frac{2r_0 h - h^2}{16\mu}\right]^{-1}\left[2r_0^2 - 2r_0 h + h^2 + \frac{2r_0 h - h^2}{\ln(1-h/r_0)}\right]^{-1}, \tag{2.3}$$

where h is the thickness of the gap between the particle and the tube walls and

$$Q = \tfrac{1}{2}r_0(U-V)$$

is the leakback.

For the flow of a neutrally buoyant particle, the particle velocity U and the mean velocity of flow V cannot be assigned independently. The resultant force on a neutrally buoyant particle due to pressures and viscous stresses exerted by the fluid must be equal to zero. Consider the equilibrium of a control volume of the suspending fluid bounded by the tube wall, the particle surface and two planes tangential to the particle at the downstream and upstream ends. Since the motion of the suspending fluid is a steady Stokes flow, the resultant of the hydrodynamic forces acting along the boundaries of the control volume must be equal to zero. A neutrally bouyant particle exerts zero force on the control volume. Thus the resultant of the pressures acting over the downstream and upstream faces of the control volume, i.e. the force due to the pressure drop, must be equal and opposite to the resultant of shear stresses acting along the tube wall (figure 1):

$$\pi r_0^2[p(-a) - p(a)] = 2\pi \int_{-a}^{a} r_0 [\tau_{Rz}]_{R=r_0}\, dz. \tag{2.4}$$

The determination of the steady-state surface shape of the particle and the stress system in the particle requires the solution of the equations of equilibrium of an elastic incompressible solid with shear modulus G,

$$\nabla^2 \mathbf{u} = G^{-1} \nabla p_s, \tag{2.5}$$

and the equation of continuity,

$$\nabla . \mathbf{u} = 0, \tag{2.6}$$

for the displacement vector $\mathbf{u}$ and the pressure p_s in the solid region.

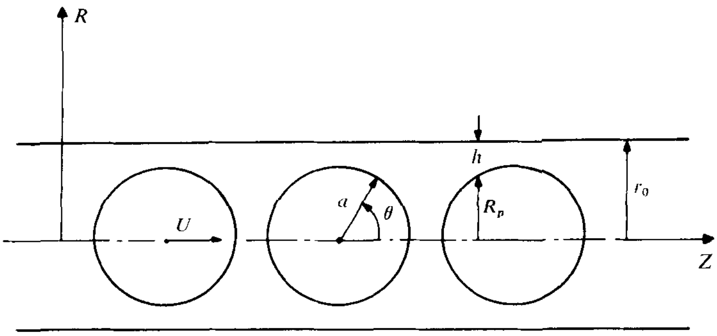

FIGURE 1. Elastic incompressible particles with a spherical shape in the unstressed state translate concentrically through a circular cylinder.

Equations (2.3)–(2.6) are coupled by the following requirements.

(i) Along the particle surface there must not be a discontinuity in the stress vector:

$$\mathbf{n}.\boldsymbol{\sigma}_s = \mathbf{n}.\boldsymbol{\sigma}_f, \tag{2.7}$$

where $\mathbf{n}$ is the unit normal vector on the surface.

(ii) The dependence of h in (2.3) and (2.4) on the surface displacements must be taken into account:

$$h = r_0 - R_p - u_R, \tag{2.8}$$

where R_p is the radial co-ordinate of the particle surface and u_R is the displacement in the R direction along the surface $R = R_p$.

The preceding equations are non-dimensionalized by introducing the following dimensionless variables and parameters:

$$\begin{aligned}
\tilde{\mathbf{r}} &= \mathbf{r}/a = \text{dimensionless position vector},\\
\tilde{\nabla} &= a\nabla = \text{dimensionless gradient operator},\\
\tilde{h} &= h/r_0 = \text{dimensionless clearance},\\
\tilde{p}_f &= p_f/G = \text{dimensionless fluid pressure},\\
\tilde{\sigma}_{ij} &= \sigma_{ij}/G = \text{dimensionless stress tensor},
\end{aligned}$$

where G is the shear modulus of the elastic particle,

$$\begin{aligned}
A &= \mu U a/G r_0^2 = \text{velocity parameter},\\
\lambda_i &= a/r_0 = \text{initial diameter ratio},\\
C &= 2Q/U r_0 = \text{leakback parameter}.
\end{aligned}$$

Upon writing (2.3) and (2.4) in terms of these dimensionless variables we obtain

$$\frac{d\tilde{p}_f}{d\tilde{z}} = 8A\left[C - \left(1 + \frac{(2-\tilde{h})\tilde{h}}{2\ln(1-\tilde{h})}\right)\right]\left(2 - 2\tilde{h} + \tilde{h}^2 + \frac{\tilde{h}(2-\tilde{h})}{\ln(1-\tilde{h})}\right)^{-1}[\tilde{h}(2-\tilde{h})]^{-1}, \tag{2.9}$$

$$\Delta\tilde{p}_f = \int_{-1}^{1}\left\{\frac{1}{2}\frac{d\tilde{p}_f}{d\tilde{z}}\left(2 + \frac{\tilde{h}(2-\tilde{h})}{\ln(1-\tilde{h})}\right) + \frac{2A}{\ln(1-\tilde{h})}\right\}d\tilde{z}. \tag{2.10}$$

The dimensionless forms of the equations of equilibrium and continuity for the elastic particle are

$$\tilde{\nabla}^2\tilde{\mathbf{u}} = \tilde{\nabla}\tilde{p}_s, \quad \tilde{\nabla}.\tilde{\mathbf{u}} = 0, \qquad (2.11), (2.12)$$

where

$$\tilde{\mathbf{u}} = \mathbf{u}/a = \text{dimensionless displacement vector,}$$

$$\tilde{p}_s = p_s/G = \text{dimensionless pressure in the solid.}$$

The system of equations (2.9)–(2.12) may be solved by a procedure of successive approximations for the unknowns: the displacement vector $\tilde{\mathbf{u}}$, the dimensionless pressures $\tilde{p}_s$ and $\tilde{p}_f$ and A or C, whichever is not specified.

In order to start the numerical iteration procedure, suppose that the steady-state surface shape of the particle is estimated. Then the Reynolds equation (2.9) and the condition (2.10) of zero drag on the particle, which is in the form of an integral equation, are readily solved to yield the pressures and viscous stresses in the fluid. The elastic particle experiences additional displacements and attains a surface shape different from the previous approximation under the action of these lubrication pressures and viscous stresses. A combination of the previous and current surface shapes which facilitates numerical stability is then adopted for the determination of the configuration at the next step of the successive approximations. The computational cycle is repeated until the additional displacements become sufficiently small and the desired degree of accuracy in the displacements is achieved.

In the remainder of this section, the formulation of the method of series solution used to evaluate the displacement field of an elastic sphere subject to stress boundary conditions is given.

It is shown by Lamb (1945, chap. 8) that (2.5) and (2.6) admit the following general solution in spherical co-ordinates $(r, \theta, \phi,)$ in a bounded region:

$$\mathbf{u} = \sum_{n=1}^{\infty}\left[\nabla\times(\mathbf{r}\chi_n) + \nabla\phi_n + \frac{n+3}{2(n+1)(2n+3)}r^2\nabla p_n - \frac{n}{(n+1)(2n+3)}\mathbf{r}p_n\right], \qquad (2.13a)$$

$$p_s = G\sum_{n=1}^{\infty} p_n, \qquad (2.13b)$$

where χ_n, ϕ_n and p_n are spherical solid harmonics of order n.

Lamb's general solution simplifies considerably for axisymmetric deformations, particularly when there is no component of displacement perpendicular to the meridian planes. Under these conditions, azimuthal displacements u_ϕ and derivatives with respect to the azimuthal angle ϕ vanish and the terms involving the solid spherical harmonic χ_n drop out. The reduced solution in dimensionless variables is

$$\tilde{u}_r = \sum_{n=1}^{\infty}\left(\frac{B_n}{a^2}n\tilde{r}^{n-1}P_n(\mu) + \frac{n}{2(2n+3)}A_n\tilde{r}^{n+1}P_n(\mu)\right), \qquad (2.14)$$

$$\tilde{u}_\theta = -\sum_{n=1}^{\infty}\left(\frac{B_n}{a^2}\tilde{r}^{n-1}(1-\mu^2)^{\frac{1}{2}}P_n'(\mu) + \frac{(n+3)\,\tilde{r}^{n+1}}{2(n+1)(2n+3)}A_n(1-\mu^2)^{\frac{1}{2}}P_n'(\mu)\right), \qquad (2.15)$$

$$\tilde{u}_\phi = 0, \qquad (2.16)$$

$$\tilde{p}_s = \sum_{n=1}^{\infty} A_n\tilde{r}^nP_n(\mu), \qquad (2.17)$$

where $\mu = \cos\theta$ and $P_n(\mu)$ is the Legendre polynomial of order n.

The stress vector $\mathbf{t}$ acting at the surface of the sphere can be shown to be (Love 1944, p. 258)

$$\mathbf{t} = \mathbf{n}.\boldsymbol{\sigma}_s = \mathbf{n}.\boldsymbol{\sigma}_f = \left\{-p_s\mathbf{e}_r + G\left(\frac{\partial\mathbf{u}}{\partial r} - \frac{\mathbf{u}}{r}\right) + \frac{G}{r}\nabla(\mathbf{r}.\mathbf{u})\right\}_{r=a}. \tag{2.18}$$

By means of (2.14)–(2.17), (2.18) can be expressed in the dimensionless form

$$\bar{t}_r = \sum_{n=1}^{\infty}\left(\frac{2B_n(n-1)n}{a^2} + \frac{n^2-n-3}{2n+3}A_n\right)P_n(\mu), \tag{2.19}$$

$$\bar{t}_\theta = -\sum_{n=1}^{\infty}\left(\frac{2B_n(n-1)}{a^2} + \frac{n(n+2)}{(n+1)(2n+3)}A_n\right)(1-\mu^2)^{\frac{1}{2}}P_n'(\mu), \tag{2.20}$$

where $\bar{\mathbf{t}} = \mathbf{t}/G$ = dimensionless traction vector acting on the surface of the particle. The interface boundary conditions (2.18) may be used to determine the unknown coefficients A_n and B_n.

Equations (2.19) and (2.20) suggest a Legendre series expansion for the radial surface traction,

$$\bar{t}_r = \sum_{n=1}^{\infty} C_n P_n(\mu), \quad C_n = \frac{2n+1}{2}\int_{-1}^{1}\bar{t}_r(\mu)P_n(\mu)\,d\mu, \tag{2.21}$$

and a Ferrer series expansion for the tangential surface traction,

$$\left.\begin{aligned}\bar{t}_\theta &= \sum_{n=0}^{\infty} D_n T_{1+n}^{-1}(\mu), \quad T_{1+n}^{-1} = \frac{\Gamma(n+1)}{\Gamma(n+3)}(1-\mu^2)^{\frac{1}{2}}P_n'(\mu),\\ D_n &= \frac{\Gamma(n+3)}{\Gamma(n+1)}\frac{2n+3}{2}\int_{-1}^{1}\bar{t}_\theta(\mu)T_{1+n}^{-1}(\mu)\,d\mu.\end{aligned}\right\} \tag{2.22}$$

In order to determine the coefficients C_n and D_n of the Legendre and Ferrer series respectively, (2.18) is used to evaluate $\bar{\mathbf{t}}$ along the interface and the relevant integrals in (2.21) and (2.22) are computed by numerical integration.

The determination of A_n and B_n reduces to the solution of the system of equations

$$\frac{2B_n n(n-1)}{a^2} + \frac{n^2-n-3}{2n+3}A_n = C_n, \quad n = 1, 2, \ldots, \tag{2.23}$$

$$\frac{2B_n(n-1)}{a^2} + \frac{n(n+2)}{(n+1)(2n+3)}A_n = -\frac{\Gamma(n+2)}{\Gamma(n)}D_{n-1}, \quad n = 1, 2, \ldots. \tag{2.24}$$

After straightforward manipulations (2.23) and (2.24) are transformed into two sets of infinite equations expressing A_n and B_n, individually, in terms of D_n and C_n. Solution of these equations, substitution in (2.14)–(2.17) and summation gives the displacement field of an elastic incompressible sphere subject to previously assigned surface tractions (2.18).

The infinite systems of linear equations are truncated after the 35th equation in order to be consistent with the 35-point Gauss–Legendre quadrature used to evaluate the coefficients C_n and D_n. There are computational errors due to truncation, the numerical integration scheme and the five-point closed integration formula based on backward differences used for the integration of the Reynolds equation. Successive approximations are terminated when three significant figures are obtained for the displacement field within the particle and for the critical gap thickness. The iterative method of solution described above is reasonably convergent if a good estimate of the steady-state surface shape of the particle is available.

3. Comparison with previous work

Lighthill (1968) and Fitz-Gerald (1969) have investigated the steady motion of tightly fitting elastic pellets in a fluid-filled circular cylindrical tube as a possible model for the flow of red blood cells in narrow capillary tubes. In this section the basic assumptions and results of these studies are discussed and compared with the present treatment.

In the studies of Lighthill (1968) and Fitz-Gerald (1969), the displacements along the surface of the particle were measured from a reference configuration that the particle was supposed to occupy initially under the application of a uniformly distributed reference pressure p_0. The shape of the particle in the reference configuration was taken to be a spheroid whose diameter perpendicular to the tube axis was equal to the diameter of the cylindrical tube. Moreover, these compressible particles were deflected radially (in the sense of cylindrical co-ordinates) by amounts proportional to the local pressures applied.

An important difference between the present treatment and the studies of Lighthill (1968) and Fitz-Gerald (1969) lies in the form of the equation expressing the condition of zero drag on the particle. Lighthill (1968) and Fitz-Gerald (1969) assumed that the force due to the pressure drop across the particle is approximately equal to the resultant of the shear stresses acting along the surface of the particle, i.e.

$$[p(-a)-p(a)]\,\pi r_0^2 = 2\pi \int_{-a}^{a} R_p\,[\tau_{Rz}]_{R=R_p}\,dz. \tag{3.1}$$

The difference between (3.1) and the exact zero-drag condition (2.4) can be shown to be significant by the use of singular asymptotic expansions derived by Bungay & Brenner (1973) for closely fitting rigid spheres.

Bungay & Brenner (1973) considered the asymmetric flow past an eccentrically located rigid sphere in a circular cylindrical tube filled with incompressible Newtonian fluid. Asymptotic expansions in terms of a perturbation parameter $\epsilon = (r_0 - a)/a$ for the hydrodynamic force on the particle on the tube wall and the pressure drop across the particle are developed for the case of Stokes flow past a stationary sphere ($U = 0$, $V \neq 0$) and for a sphere translating through an otherwise quiescent fluid ($U \neq 0$, $V = 0$), where U and V are the particle and average flow velocities respectively.

For a concentrically positioned sphere, the force $\Delta p A$ due to the pressure drop across the particle is given by Bungay & Brenner (1973) as

$$\Delta p_t A = -\tfrac{9}{4} \times 2^{\frac{1}{2}}\pi^2 \mu a U \epsilon^{-\frac{5}{2}} \left(1 + \frac{157}{60}\,\epsilon + \frac{101093}{50400}\,\epsilon^2\right) + O(1) \tag{3.2}$$

when $U \neq 0$, $V = 0$ and $\epsilon \to 0$ and as

$$\Delta p_s A = \tfrac{9}{4} \times 2^{\frac{1}{2}}\pi^2 \mu a V \epsilon^{-\frac{5}{2}} \left(1 + \frac{79}{20}\epsilon + \frac{301573}{50400}\,\epsilon^2\right) + O(1) \tag{3.3}$$

when $U = 0$, $V \neq 0$ and $\epsilon \to 0$, where μ is the fluid viscosity, a is the particle radius and

$A = \pi r_0^2$. The subscripts t and s indicate, respectively, the cases (i) $U \neq 0$, $V = 0$ and (ii) $U = 0$, $V \neq 0$.

The resultant force F^w due to shear stresses acting along the tube wall is evaluated by Bungay (1970):

$$F_t^w = -3 \times 2^{\frac{1}{2}} \pi^2 \mu a U \epsilon^{-\frac{3}{2}} (1 + \tfrac{19}{60}\epsilon) + O(1) \tag{3.4}$$

when $U \neq 0$, $V = 0$ and $\epsilon \to 0$;

$$F_s^w = 3 \times 2^{\frac{1}{2}} \pi^2 \mu a V \epsilon^{-\frac{3}{2}} (1 + \tfrac{179}{60}\epsilon) + O(1) \tag{3.5}$$

when $U = 0$, $V \neq 0$ and $\epsilon \to 0$.

Since the governing differential equations and the boundary conditions are linear, the asymptotic expansions for the pressure drop and the resultant of the shear on the tube evaluated for the cases (i) $U = 0$, $V \neq 0$ and (ii) $U \neq 0$, $V = 0$ can be superposed to obtain the corresponding expansions for more general flow conditions, i.e. $U \neq 0$, $V \neq 0$. In particular, for the case of a neutrally buoyant particle, the zero-drag condition (2.4) may be used to determine the mean flow velocity in terms of the particle velocity in the series form

$$V = U(1 - \tfrac{4}{3}\epsilon + \tfrac{46}{15}\epsilon^2) + O(\epsilon^{\frac{5}{2}}). \tag{3.6}$$

Substitution of (3.6) into (3.3) and the addition of (3.2) yield the force due to the pressure drop across the neutrally buoyant particle:

$$\Delta p_n A = 4 \times 2^{\frac{1}{2}} \pi^2 \mu a U \epsilon^{-\frac{1}{2}} + O(1), \tag{3.7}$$

where subscript n indicates that the rigid sphere is taken to be neutrally buoyant.

The use of (3.1), which was formulated by Lighthill (1968) to represent the condition of zero drag on the particle, instead of (2.4) yields an asymptotic expansion for the force due to the pressure drop across the particle which is substantially different from (3.7). In order to establish the explicit relationship between U and V by the use of (3.1), it is essential that the asymptotic expansions for the resultant F^s of the shear stresses acting along the particle for the cases (i) $U \neq 0$, $V = 0$ and (ii) $U = 0$, $V \neq 0$ be determined:

$$F^s = 2\pi \int_{-a}^{a} R_p \, [\tau_{Rz}]_{R=R_p} \, dz. \tag{3.8}$$

Calculations of the hydrodynamic force on the particle due to pressures and viscous stresses have been carried out by Bungay (1970), however the contribution of shear stresses alone has not been presented separately. For the present purposes, we have used the asymptotic expansions developed by Bungay (1970) for the velocity components to determine the shear stresses acting along the surface of the particle and performed the integration in (3.8) to obtain

$$F_t^s = 3 \times 2^{\frac{1}{2}} \pi^2 \mu a U \epsilon^{-\frac{3}{2}} (-1 + \tfrac{173}{30}\epsilon) + O(1) \tag{3.9}$$

when $U \neq 0$, $V = 0$ and $\epsilon \to 0$ and

$$F_s^s = 3 \times 2^{\frac{1}{2}} \pi^2 \mu a V \epsilon^{-\frac{3}{2}} (1 - \tfrac{133}{30}\epsilon) + O(1) \tag{3.10}$$

when $U = 0$, $V \neq 0$ and $\epsilon \to 0$. Equations (3.9) and (3.10) are substituted into (3.1) in order to determine the mean flow velocity in this case:

$$V = U(1 - \tfrac{4}{3}\epsilon + \tfrac{406}{315}\epsilon^2) + O(\epsilon^{\frac{5}{2}}) \quad \text{as} \quad \epsilon \to 0. \tag{3.11}$$

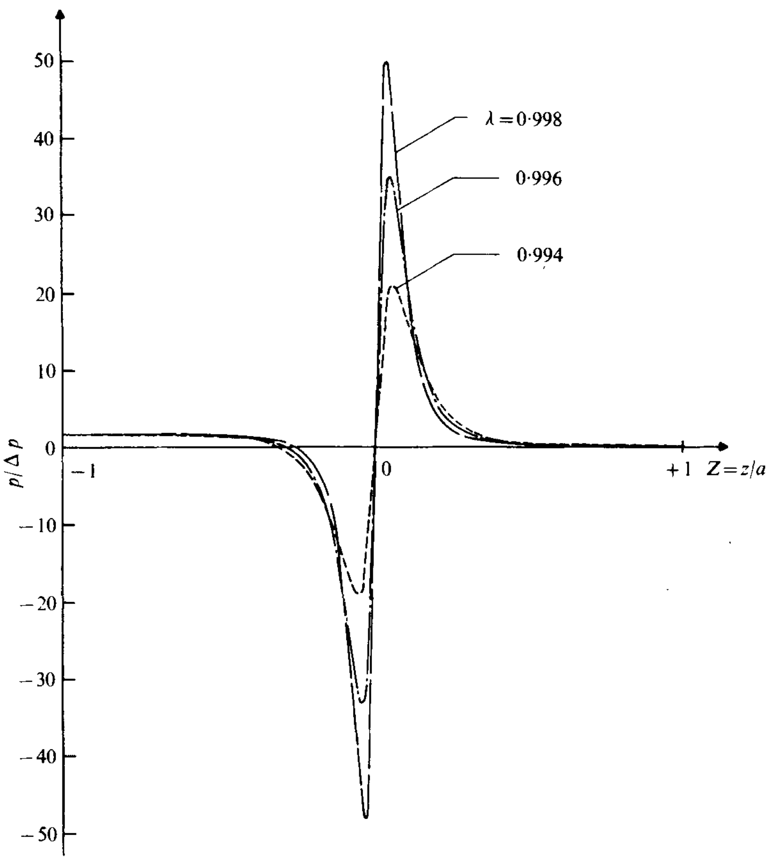

FIGURE 2. Pressure distributions along the surface of rigid spherical particles computed by lubrication theory. The pressure is normalized with Δp, the pressure drop across the particle.

λ	$\tilde{F}^p$	$\tilde{F}^w$	$\tilde{F}^s$
0·994	607·9	608·2	79·0
0·996	768·7	768·5	84·2
0·998	1125·3	1124·8	107·1

$$\tilde{F}^p = \pi r_0^2[\mu a U]^{-1}[p(-a)-p(a)]$$

$$\tilde{F}^w = 2\pi[\mu a U]^{-1}\int_{-a}^{a} r_0[\tau_{Rz}]_{R=r_0}\,dz$$

$$\tilde{F}^s = 2\pi[\mu a U]^{-1}\int_{-a}^{a} R_p[\tau_{Rz}]_{R=R_p}\,dz$$

TABLE 1. Rigid-particle parameters.

Then the force due to the pressure drop across the particle is found by superposition as

$$\Delta p_n A = O(1) \quad \text{as} \quad \epsilon \to 0. \tag{3.12}$$

The discrepancy between (3.7) and (3.12) is due to the neglect of the effects of rapidly varying pressures in the vicinity of the minimum gap thickness by Lighthill (1968) and Fitz-Gerald (1969). These pressures act over a length $o(1)$. However, they exert a

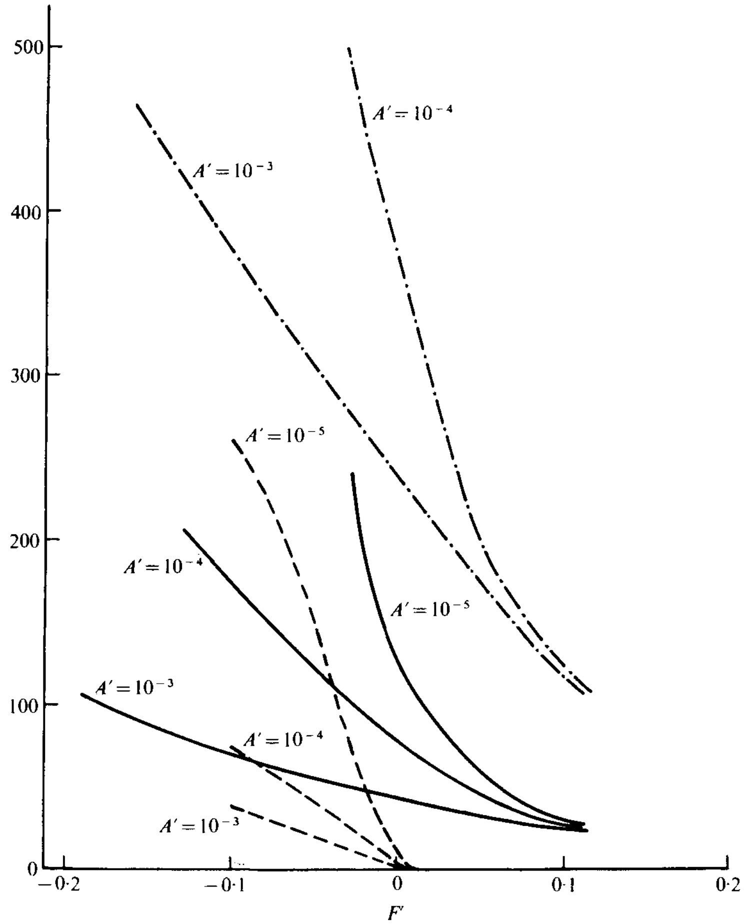

FIGURE 3. Comparison of D' *vs.* F' curves for several different values of A': ----, Lighthill (1968); –·–·–, Fitz-Gerald (1969); ——, corresponding curves obtained by the application of their theory with the corrected zero-drag condition.

resultant force $O(\epsilon^{-\frac{1}{2}})$ on the particle in the axial direction (see figure 2). To demonstrate some typical numerical values, lubrication theory has been used to calculate the force $\tilde{F}^p$ due to the pressure drop, the resultant force $\tilde{F}^w$ on the tube wall and the force $\tilde{F}^s$ on the particle due to shear stresses in dimensionless form for rigid spheres of various sizes. Some sample results are given in table 1. These numerical values agree well with predictions obtained from the above asymptotic analysis using (3.4)–(3.10).

It is interesting to compare the results of the studies of Lighthill (1968) and Fitz-Gerald (1969) and a modified theory where (3.1) is replaced by (2.4). It is convenient to introduce several dimensionless parameters defined by Lighthill (1968) and Fitz-Gerald (1969):

$$B' = \beta[p(a)-p_0]/r_0 = \text{clearance parameter},$$

$$F' = \beta[\tfrac{1}{2}(p(a)+p(-a))-p_0]/r_0 = \text{clearance parameter},$$

$$A' = \mu U\beta/r_0^2(kr_0)^{\frac{1}{2}} = \text{velocity parameter},$$

$$D' = [p(-a)-p(a)]\,r_0(kr_0)^{\frac{1}{2}}/\mu U = \text{resistance parameter},$$

where μ is the viscosity of the fluid, β is the compliance of the flexible particle and k is the eccentricity of the elliptical cross-section. The resistance parameter D' is equal to one-sixteenth of the ratio of the pressure drop across the particle to the pressure drop in Poiseuille flow with mean velocity U. Figure 8 of Lighthill (1968) shows D' *vs.* B' curves for several constant values of A'. For positive clearance ($B' > 0$) very low resistances ($D' < 16$), smaller than the resistance experienced by the equivalent Poiseuille flow, are predicted which are not possible for a suspension of solid particles (Skalak 1970).

Figure 3 shows D' *vs.* F' curves for constant values of A' computed using the zero-drag condition (2.4). Also shown in figure 3 for comparison are curves from figure 8 of Lighthill (1968) and figure 4 of Fitz-Gerald (1969) for the same values of A'. Figure 3 shows that the pressure differences predicted by Lighthill are always less than the values evaluated with the use of (2.4) for comparable parameter values. The reasons for the disagreement are clear from the asymptotic analysis given earlier in this section.

In the shear-stress expression used by Fitz-Gerald (1969, equation 3.6) there is also an error in sign. This caused an overestimation of the resultant of the shear stresses on the particle. As a result, unrealistically high values of the additional pressure drop per particle are predicted in all cases as can be seen in figure 3.

4. Numerical results and discussion

This section is concerned with the numerical results obtained from the theory developed in §2, in which each particle is considered as an elastic continuum. The initial diameter ratio $\lambda_i = a/r_0$ and the velocity parameter $A = \mu Ua/Gr_0^2$, which incorporates the effects of the particle velocity U, the viscosity of the suspending fluid μ and the shear modulus of the elastic particle G, are chosen as the independent parameters. The deformations of the elastic particle and the state of stress in the fluid and solid phases are determined for various values of λ_i and A.

It is expedient to present the numerical results in terms of dimensionless variables. The relative apparent viscosity η will be used to represent the pressure drop Δp over a length Δz including one particle. The particle spacing is taken to be equal to one particle diameter $2a$. The relative apparent viscosities computed thus apply to a line of spheres in contact with each other. Accordingly

$$\eta = \Delta p/(16\mu Va/r_0^2), \tag{4.1}$$

where the denominator $16\mu Va/r_0^2$ is the pressure drop in a length $2a$ of a Poiseuille flow of the suspending fluid with the same mean velocity V in the absence of suspended particles.

Lubrication theory, which is assumed to be valid here, predicts Poiseuille flow in the space between the particles. Under this approximation, the relative apparent viscosities for arbitrary particle spacings may be obtained by averaging the results given here for a line of spheres which are just touching each other with $\eta = 1$ for the length in which the particles are absent.

The results for the elastic deformation of the particle are given in terms of the final diameter ratio λ_f, which is defined as the ratio of the maximum radius of the deformed particle to the tube radius. Finite deformations of the elastic particle are not treated by

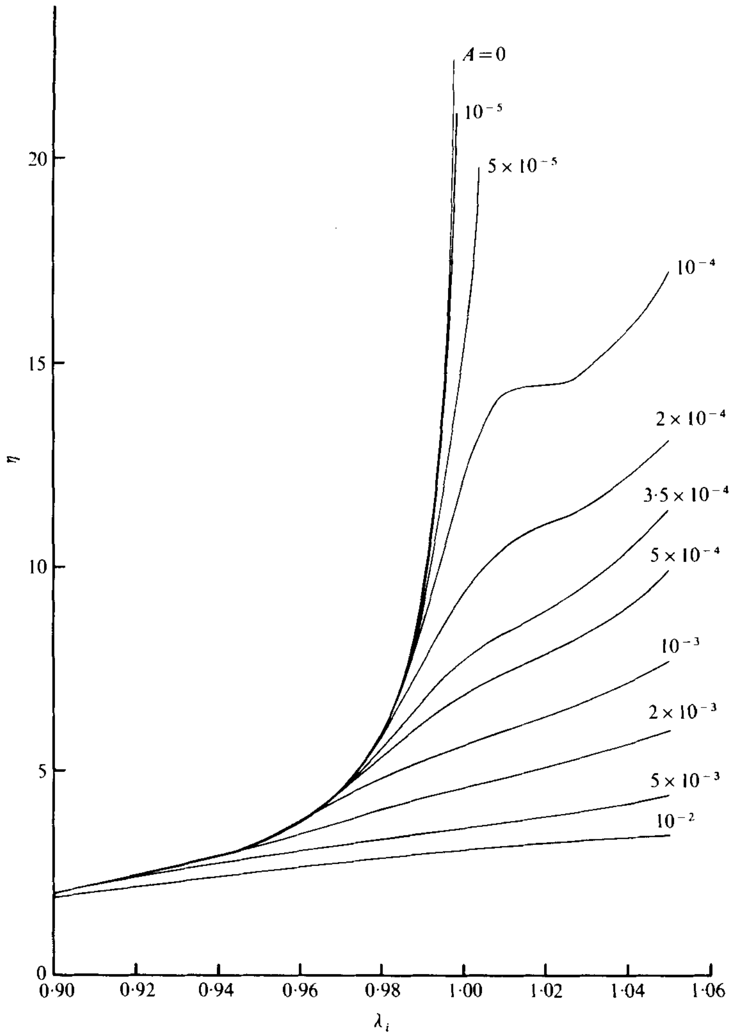

FIGURE 4. Relative apparent viscosity η *vs.* initial diameter ratio λ_i for various values of the velocity parameter A. The spacing between particles is one particle diameter $d = 2a$. Each particle is an elastic sphere.

the present theory, which is based on the assumptions of the linear theory of elasticity. Hence solutions are sought in the ranges $0{\cdot}9 < \lambda_i < 1{\cdot}05$ and $0 < A < 10^{-3}$. Deformations are then of the order of 5 %.

Figure 4 shows the relative apparent viscosity η as a function of the initial diameter ratio λ_i for several values of the velocity parameter A. The curve $A = 0$ gives the solutions for a rigid sphere. All of the curves A = constant approach each other for initial diameter ratios λ_i below 0·96. For smaller initial diameter ratios there is very little deformation of the particles for the range of A assumed. For higher values of λ_i, the curves for different values of A separate and elastic deformations of the particle become an important factor in the determination of the flow and pressure characteristics of the suspension.

Figure 5 shows the final diameter ratio of the particle λ_f plotted against the initial

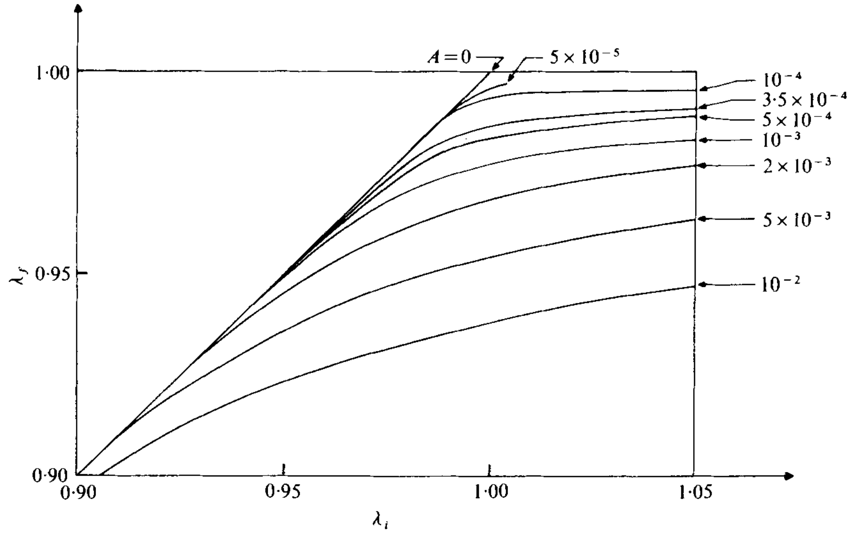

FIGURE 5. Final diameter ratio λ_f *vs.* initial diameter ratio λ_i for several values of the velocity parameter A. The particle spacing is one particle diameter $d = 2a$. Each particle is an elastic sphere.

λ_i	λ_f	η	C
0·980	0·9796	5·83	0·02624
0·990	0·9878	8·34	0·01387
0·995	0·9911	10·10	0·01175
1·000	0·9934	11·86	0·00905
1·008	0·9943	14·07	0·00772
1·015	0·9946	14·41	0·00769
1·029	0·9948	14·79	0·00766
1·044	0·9952	16·03	0·00737
1·050	0·9958	17·20	0·00705

TABLE 2. Elastic-particle parameters: relative apparent viscosity η, final diameter ratio λ_f and leakback parameter C for $A = 10^{-4}$ and various values of initial diameter ratio λ_i (see the pressure curves, figure 7).

diameter ratio λ_i for various A. When the maximum radius of the deformed particle is almost equal to the radius of the tube (see curve for $A = 5\times10^{-5}$ in figure 5), η (see figure 4) tends to infinity very rapidly. For sufficiently large values of A and λ_i, the curves of λ_f in figure 5 may intersect $\lambda_f = 1$ at a finite value of λ_i. Then η may approach infinity along a curve A = constant with a vertical asymptote passing through this particular value of λ_i in figure 4 (see curve for $A = 5\times10^{-5}$ in figure 4). It has been suggested by Lighthill (1968) that a similar phenomenon is possible in capillary blood flow, namely that velocities below a certain minimum value cannot be attained in sufficiently narrow capillaries because of the failure of the hydrodynamic lubrication and consequent seizing up of the red blood cells. The results of the present study support the possibility of this phenomenon.

In figure 6, η is shown as a function of A for several values of λ_i. For $\lambda_i \leqslant 0\cdot98$, over a wide range of A, η remains nearly constant along curves λ_i = constant since there are

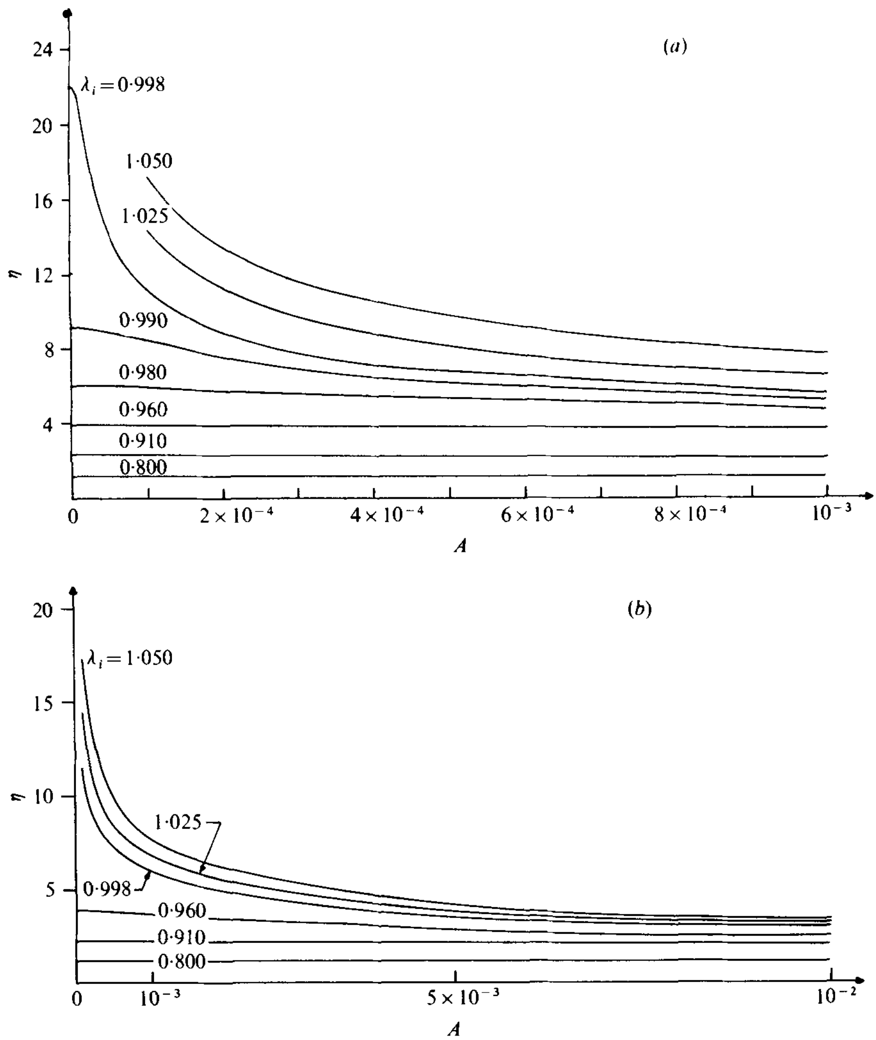

FIGURE 6. (a) Relative apparent viscosity η computed for a line of elastic spheres with a uniform spacing of one particle diameter as a function of the velocity parameter A for several values of the initial diameter ratio λ_i. (b) Curves λ_i = constant for a wider range of the velocity parameter: $0 < A < 10^{-2}$.

essentially no elastic deformations. However, for closely fitting particles and particularly when the diameter of the particle is greater than the diameter of the tube, η is strongly dependent on the velocity parameter A and initial diameter ratio λ_i.

Figure 7 shows dimensionless pressure curves for $A = 10^{-4}$ and several values of the initial diameter ratio λ_i. The corresponding dimensionless parameters are listed in table 2. In the range $1{\cdot}008 < \lambda_i < 1{\cdot}05$, the variations in relative apparent viscosity are small (see figure 4); however, the pressure curves in figure 7 differ significantly for different values of λ_i. The curves in figure 7 for elastic particles are seen to be less symmetric than those for rigid spheres shown in figure 2. This is typical for elastic particles.

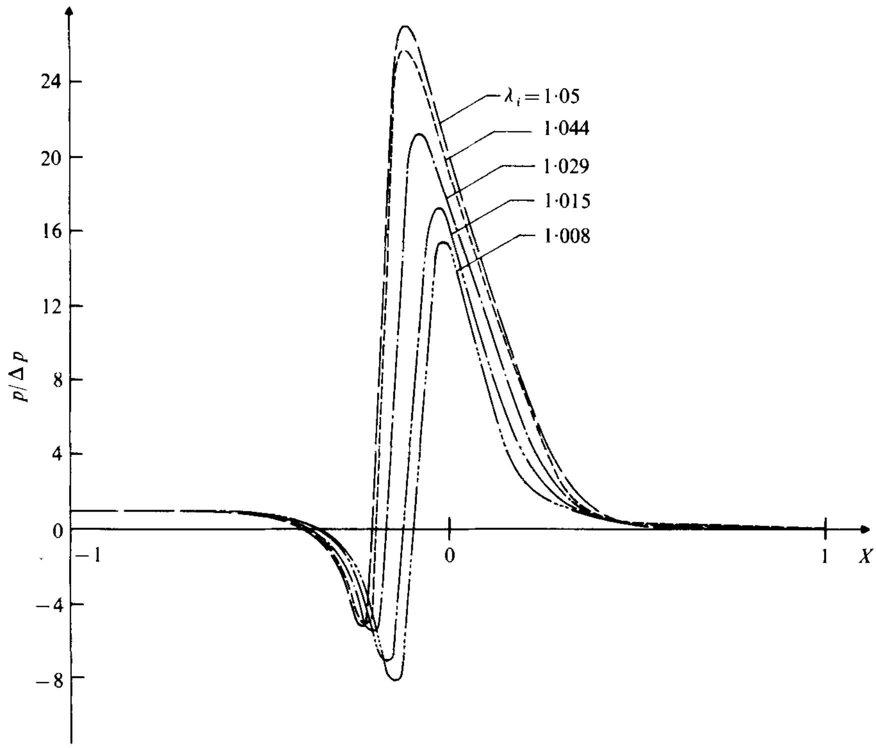

FIGURE 7. Dimensionless pressure curves for $A = 10^{-4}$ and several values of the initial diameter ratio λ_i. The relevant dimensionless parameters are listed in table 2. Compare this figure with figure 2, which is for rigid spheres.

The numerical results presented above have not yet been confirmed by any detailed experiments, but could perhaps be verified by using rubber spheres in oil-filled tubes. For either red or white blood cells, exact measurements are not feasible because of the extremely small clearances involved. However, the qualitative results may be used to interpret gross measurements of apparent viscosities and to make theoretical predictions for networks of capillaries.

This work was supported by U.S. National Institutes of Health under Program Project HL-16851. Dr Shu Chien is the Director of the Program Project and his advice and encouragement are gratefully acknowledged.

Addendum, by M. J. Lighthill

I am most grateful to Dr Tözeren and Dr Skalak for pointing out correctly the many unsatisfactory features of the mathematical model originated by Lighthill (1968). Over the past decade, I had myself increasingly come to appreciate the model's complete lack of any quantitative value, and I welcome the opportunity to affirm this. I should remark at the same time that the essential qualitative nature of the theoretical approach to blood flow in capillaries, which was all I described in my book (*Mathematical Biofluiddynamics*, SIAM, 1975, chap. 14), remains correct. Excess pressures in lubricating layers of small thickness h are of order $\mu U/h^2$. These can generate the required large deformation of a red blood cell moving at speed U in a very narrow capillary if and only if the thickness h varies as $U^{\frac{1}{2}}$. The required pressure drop is of order $\mu U/h$ and therefore also varies as $U^{\frac{1}{2}}$. As noted in the book, a substantial measure of observational evidence supports these qualitative statements.

REFERENCES

AROESTY, J. & GROSS, J. F. 1970 Convection and diffusion in the microcirculation. *Microvasc. Res.* **2**, 247–267.

BAGGE, U. 1975 White blood cell rheology. Ph.D. dissertation, University of Gothenburg, Sweden.

BUGLIARELLO, G. & HSIAO, C. C. 1967 Numerical simulation of three-dimensional flow in the axial plasmatic gaps of capillaries. *7th Int. Cong. Med. Biol. Engng, Stockholm, Sweden.*

BUNGAY, P. M. 1970 The motion of closely-fitting particles through fluid-filled tubes. Ph.D. dissertation, Carnegie-Mellon University, Pittsburgh.

BUNGAY, P. M. & BRENNER, H. 1973 The motion of a closely-fitting sphere in a fluid filled tube. *Int. J. Multiphase Flow* **1**, 25–56.

CHEN, T. C. & SKALAK, R. 1970 Spheroidal particle flow in a cylindrical tube. *Appl. Sci. Res.* **22**, 403–441.

COKELET, G. R. 1976 Macroscopic rheology and tube flow of human blood. In *Microcirculation*, vol. 1 (ed. J. Grayson & W. Zingg), pp. 29–52. Plenum.

FITZ-GERALD, J. M. 1969 Mechanics of red-cell motion through very narrow capillaries. *Proc. Roy. Soc.* B **174**, 193–227.

HOCHMUTH, R. M. & SUTERA, S. P. 1970 Spherical caps in low Reynolds number tube flow. *Chem. Engng Sci.* **25**, 593–604.

HYMAN, W. A. & SKALAK, R. 1972 Non-Newtonian behaviour of a suspension of liquid drops in fluid flow. *A.I.Ch.E. J.* **18**, 149–154.

LAMB, H. 1945 *Hydrodynamics*, 6th edn. Dover.

LEW, H. S. & FUNG, Y. C. 1969 The motion of the plasma between the red cells in the bolus flow. *Biorheol.* **6**, 109–119.

LIGHTHILL, M. J. 1968 Pressure-forcing of tightly fitting pellets along fluid-filled elastic tubes. *J. Fluid Mech.* **34**, 113–143.

LOVE, A. E. H. 1944 *A Treatise of the Mathematical Theory of Elasticity*, 4th edn. Dover.

SKALAK, R. 1970 Extensions of extremum principles for slow viscous flows. *J. Fluid Mech.* **42**, 527–548.

SKALAK, R., CHEN, P. H. & CHIEN, S. 1972 Effect of hematocrit and rouleaux on apparent viscosity in capillaries. *Biorheol.* **9**, 67–82.

SUTERA, S. P. & HOCHMUTH, R. M. 1968 Large scale modelling of blood flow in the capillaries. *Biorheol.* **5**, 45–73.

SUTERA, S. P., SESHADRI, P. A. & HOCHMUTH, R. M. 1970 Capillary blood flow: II. Deformable model cells in tube flow. *Microvasc. Res.* **2**, 420–433.

WANG, H. & SKALAK, R. 1969 Viscous flow in a cylindrical tube containing a line of spherical particles. *J. Fluid Mech.* **38**, 75–96.

ZARDA, P. R., CHIEN, S. & SKALAK, R. 1977*a* Elastic deformation of red blood cells. *J. Biomech.* **10**, 211–221.

ZARDA, P. R., CHEIN, S. & SKALAK, R. 1977*b* Interaction of a viscous incompressible fluid with an elastic body. *Symp. Fluid–Structure Interaction.* New York: A.S.M.E.